

NAVAL POSTGRADUATE SCHOOL

Monterey, California



THESIS

COMPUTERIZED BALLISTIC MODELING OF THE COMANCHE TAILFAN SHROUD

by

Allen H. Stephan

December 2000

Thesis Advisor:
Co-Advisor:

E. Roberts Wood
Donald A. Danielson

Approved for public release; distribution is unlimited

20010320 039

REPORT DOCUMENTATION PAGE		Form Approved OMB No. 0704-0188	
Public reporting burden for this collection of information is estimated to average 1 hour per response, including the time for reviewing instruction, searching existing data sources, gathering and maintaining the data needed, and completing and reviewing the collection of information. Send comments regarding this burden estimate or any other aspect of this collection of information, including suggestions for reducing this burden, to Washington headquarters Services, Directorate for Information Operations and Reports, 1215 Jefferson Davis Highway, Suite 1204, Arlington, VA 22202-4302, and to the Office of Management and Budget, Paperwork Reduction Project (0704-0188) Washington DC 20503.			
1. AGENCY USE ONLY (Leave blank)		2. REPORT DATE December 2000	3. REPORT TYPE AND DATES COVERED Master's Thesis
4. TITLE AND SUBTITLE: Title (Mix case letters) Computerized Ballistic Modeling of the Comanche Tailfan Shroud		5. FUNDING NUMBERS	
6. AUTHOR(S) Stephan, Allen H.		8. PERFORMING ORGANIZATION REPORT NUMBER	
7. PERFORMING ORGANIZATION NAME(S) AND ADDRESS(ES) Naval Postgraduate School Monterey, CA 93943-5000		10. SPONSORING / MONITORING AGENCY REPORT NUMBER	
9. SPONSORING / MONITORING AGENCY NAME(S) AND ADDRESS(ES) N/A		10. SPONSORING / MONITORING AGENCY REPORT NUMBER	
11. SUPPLEMENTARY NOTES The views expressed in this thesis are those of the author and do not reflect the official policy or position of the Department of Defense or the U.S. Government.			
12a. DISTRIBUTION / AVAILABILITY STATEMENT Approved for public release; distribution is unlimited		12b. DISTRIBUTION CODE	
13. ABSTRACT (maximum 200 words) The U.S. Army has contracted Boeing-Sikorsky to develop the RAH-66 Comanche, a new, armed reconnaissance helicopter that features stealth technology designed to improve survivability when operating in hostile environments. Ballistic testing is required on the Comanche prior to fielding. Computer based simulations are being employed in order to reduce requirements for expensive live-fire testing. This thesis uses a computer program called Dytran from MacNeal-Schwendler to simulate the effects of an explosive round detonating in the Comanche tailfan shroud. Six test cases involving explosions with varying amounts of explosive energy, or specific internal energy, are evaluated. From these tests, a curve showing the percentage of structural failure versus the specific internal energy is plotted. Assuming that 20% structural failure of the model equates to a catastrophic failure, this analysis shows that the analyzed section of the Comanche tailfan shroud can withstand an explosion with a specific internal energy of $2.58 * 10^{10} \text{ in}^2/\text{sec}^2$. Any potential threat rounds with specific internal energies greater than $2.58 * 10^{10} \text{ in}^2/\text{sec}^2$ will pose serious threats to the Comanche.			
14. SUBJECT TERMS Comanche, Ballistic Modeling, Dytran, Tailfan Shroud			15. NUMBER OF PAGES 64
			16. PRICE CODE
17. SECURITY CLASSIFICATION OF REPORT Unclassified	18. SECURITY CLASSIFICATION OF THIS PAGE Unclassified	19. SECURITY CLASSIFICATION OF ABSTRACT Unclassified	20. LIMITATION OF ABSTRACT UL

THIS PAGE INTENTIONALLY LEFT BLANK

Approved for public release; distribution is unlimited

**COMPUTERIZED BALLISTIC MODELING OF THE COMANCHE TAILFAN
SHROUD**

Allen H. Stephan
Captain, United States Army
B.S., United States Military Academy, 1991

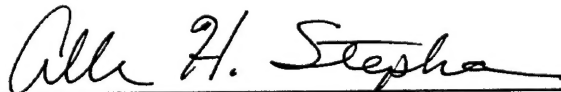
Submitted in partial fulfillment of the
requirements for the degree of

MASTER OF SCIENCE IN AERONAUTICAL ENGINEERING

from the

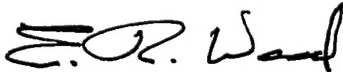
**NAVAL POSTGRADUATE SCHOOL
December 2000**

Author:

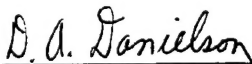


Allen H. Stephan

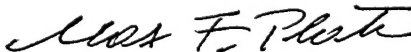
Approved by:



E. Roberts Wood, Thesis Advisor



Donald A. Danielson, Co-Advisor



Max F. Platzer, Chairman
Department of Aeronautics and Astronautics

THIS PAGE INTENTIONALLY LEFT BLANK

ABSTRACT

The U.S. Army has contracted Boeing-Sikorsky to develop the RAH-66 Comanche, a new, armed reconnaissance helicopter that features stealth technology designed to improve survivability when operating in hostile environments. Ballistic testing is required on the Comanche prior to fielding. Computer based simulations are being employed in order to reduce requirements for expensive live-fire testing. This thesis uses a computer program called Dytran from MacNeal-Schwendler to simulate the effects of an explosive round detonating in the Comanche tailfan shroud. Six test cases involving explosions with varying amounts of explosive energy, or specific internal energy, are evaluated. From these tests, a curve showing the percentage of structural failure versus the specific internal energy is plotted. Assuming that 20% structural failure of the model equates to a catastrophic failure, this analysis shows that the analyzed section of the Comanche tailfan shroud can withstand an explosion with a specific internal energy of $2.58 * 10^{10} \text{ in}^2/\text{sec}^2$. Any potential threat rounds with specific internal energies greater than $2.58 * 10^{10} \text{ in}^2/\text{sec}^2$ will pose serious threats to the Comanche.

THIS PAGE INTENTIONALLY LEFT BLANK

TABLE OF CONTENTS

I.	INTRODUCTION	1
A.	GENERAL.....	1
B.	SCOPE.....	2
C.	STATEMENT OF PURPOSE.....	3
II.	BACKGROUND.....	5
A.	FINITE ELEMENT METHOD.....	5
B.	COMPUTER SOFTWARE.....	6
1.	IDEAS.....	6
2.	Dytran	6
3.	Patran	7
C.	BLAST MECHANICS.....	7
D.	COMPOSITE MATERIALS.....	8
III.	MODEL DEVELOPMENT	11
A.	OVERVIEW	11
B.	CATIA TRANSLATION	13
C.	MODEL CLEANUP.....	13
D.	MESHING.....	14
E.	FINAL MODEL CHECKS.....	15
F.	WRITING DYTRAN DECKS	16
IV.	EXPERIMENTAL RESULTS.....	17
A.	ASSUMPTIONS USED IN ANALYSIS	17
B.	OVERVIEW	18
C.	TEST 1 RESULTS	20
D.	TEST 2 RESULTS	20
E.	TEST 3 RESULTS	21
F.	TEST 4 RESULTS	21
G.	TEST 5 RESULTS	22
H.	TEST 6 RESULTS	23
I.	MAXIMUM BLAST ENERGY STRUCTURE CAN WITHSTAND.....	24
V.	CONCLUSIONS AND RECOMMENDATIONS.....	27
A.	CONCLUSIONS	27
B.	RECOMMENDATIONS.....	27
	LIST OF REFERENCES	29
	INITIAL DISTRIBUTION LIST	31

THIS PAGE INTENTIONALLY LEFT BLANK

LIST OF FIGURES

Figure 1: RAH-66 Comanche [From 1]	1
Figure 2: Schematic View of Blast Analysis Area.....	3
Figure 3: Left Side View of Model of Analysis Area	11
Figure 4: Top View of Model of Analysis Area with Top Plate Removed.....	11
Figure 5: Plot of Maximum Strain vs. Time for All Test Cases	18
Figure 6: Maximum Strain Area from Initial Blast Wave	19
Figure 7: Maximum Strain for Test Case #1 ($SIE = 10^{10} \text{ in}^2/\text{sec}^2$).....	20
Figure 8: Maximum Strain for Test Case #2 ($SIE = 1.3 * 10^{10} \text{ in}^2/\text{sec}^2$).....	20
Figure 9: Maximum Strain for Test Case #3 ($SIE = 2.5 * 10^{10} \text{ in}^2/\text{sec}^2$).....	21
Figure 10: Maximum Strain from Initial Blast Wave for Test Case #4 ($SIE = 3.8 * 10^{10} \text{ in}^2/\text{sec}^2$)	21
Figure 11: Maximum Strain for Test Case #4 ($SIE = 3.8 * 10^{10} \text{ in}^2/\text{sec}^2$).....	22
Figure 12: Maximum Strain for Test Case #5 ($SIE = 5 * 10^{10} \text{ in}^2/\text{sec}^2$).....	22
Figure 13: Maximum Strain from Initial Blast Wave for Test Case #6 ($SIE = 10^{11} \text{ in}^2/\text{sec}^2$).....	23
Figure 14: Maximum Strain for Test Case #6 ($SIE = 10^{11} \text{ in}^2/\text{sec}^2$).....	23
Figure 15: Plot of Percentage of Failed Structure vs. SIE	25

LIST OF TABLES

Table 1: Failure Data for Each Cycle.....	24
---	----

THIS PAGE INTENTIONALLY LEFT BLANK

ACKNOWLEDGEMENTS

I would like to acknowledge the financial support of Boeing Helicopters in Philadelphia, PA. The Boeing Company paid my temporary living expenses while I was in Philadelphia developing the model used in this analysis thus making this thesis possible. I would like to thank everyone at Boeing who helped with this project. A special thanks goes to Mel Niederer, Jason Firko and Agnes Wozniak who took the time to answer my numerous questions, provided their friendship, and made my experience at Boeing truly special. I would also like to thank Professors Bob Wood and Don Danielson for their support, guidance and encouragement during this process. They always seemed to find the time to answer my questions and provide advice in order to keep the project moving forward. Finally, I would like to thank Terri, Meagan and Jake, my wife and children, for their love, understanding and support which kept me going during this undertaking.

THIS PAGE INTENTIONALLY LEFT BLANK

I. INTRODUCTION

A. GENERAL

On June 1, 2000, the United States Army and Boeing-Sikorsky officials launched the \$3.1 Billion Engineering and Manufacturing Development (EMD) phase of the RAH-66 Comanche. The EMD contract calls for Boeing-Sikorsky to deliver a total of thirteen aircraft. The first four will be delivered in 2005 while the remaining nine aircraft will be delivered in 2006. The EMD aircraft are part of the 1,213 aircraft the Army is planning to buy from Boeing-Sikorsky. Currently, two technology demonstrators have been built and are undergoing testing. One of these aircraft is pictured below:



Figure 1: RAH-66 Comanche [From 1]

Comanche is an armed reconnaissance helicopter with projected missions of armed reconnaissance, light attack and air combat. Comanche capabilities are those demanded of a smaller force structure. They include improved mobility, increased survivability and dramatically reduced operation and support costs. The Comanche's most significant systems and features include: [From 2]

- Twin Turbine Engines

- Two member crew
- Five-bladed bearingless main rotor
- FANTAIL anti-torque system
- Advanced digital mission electronics and sensors
- Longbow fire-control radar (Fire and Forget Capability)
- Low observables (radar, infrared, acoustic)
- On-board diagnostic system with simple remove-and-replace maintenance
- Internal armament storage
- Stowable 20-mm Gatling gun

B. SCOPE

Ballistic survivability is a major concern for modern military vehicles. To meet combat requirements, Comanche is required to undergo ballistic testing prior to fielding. Because the aircraft is usually destroyed in testing, ballistic testing can be extremely expensive. Therefore, to reduce program acquisition costs for new military vehicles, the amount of ballistic testing is being reduced wherever possible and new, less expensive validation methods are being introduced. One of the most promising new validation techniques is based upon computer simulations instead of actual destructive testing. A major advantage of a computer simulation over actual testing is that the computer model does not get destroyed and can be reused as often as required. Additionally, changing parameters in the computer is significantly easier than changing parameters on physical models thus making design optimization easier.

C. STATEMENT OF PURPOSE

The goal of this research is to determine how large of an explosion is required to cause a catastrophic failure in the shaded section of Comanche tailfan shroud shown in Figure 2.

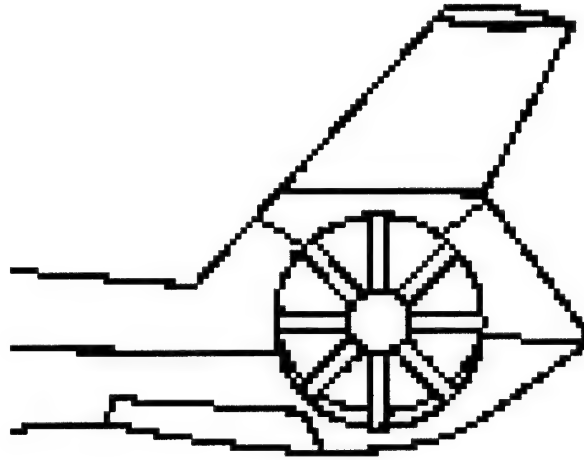


Figure 2: Schematic View of Blast Analysis Area

The explosion analyzed in this thesis models the detonation of an explosive round after impacting the tailfan shroud structure. Strength of the explosive round is measured in terms of energy per mass and is described by the term Specific Internal Energy (SIE). The higher the SIE of an explosive round, the more powerful the explosion that round creates when detonated.

Six cases involving explosions with varying SIE values will be evaluated. The computer analysis determines which portions of the structural model fail as a result of the explosion. The structure failure data is evaluated to determine the maximum SIE value the tailfan shroud can withstand before catastrophically failing. Catastrophic failure is the inability of the structure to carry flight loads.

THIS PAGE INTENTIONALLY LEFT BLANK

II. BACKGROUND

A. FINITE ELEMENT METHOD

Modern aircraft, like the Comanche, are complex assemblies of structural components. The response of these structural components can be determined by analysis methods that include beam bending, torsion, and shear flow. Complex structures, like those seen in Comanche, are difficult to analyze with these classical, continuous methods. To simplify analysis of such complex structures, the Finite Element Method (FEM) was introduced in the late 1950's. [From 3]

The FEM reduces complex structures to an assembly of discrete elements like beams, plates, and solids. Dynamic response for each of these elements is now more easily solved when compared to the analysis of the complete structure. To summarize, the complete structure is broken down into elements, each element is analyzed separately for equilibrium, and the structure is tied back together by imposing compatibility requirements (on displacements) or equilibrium (on forces) at the joints or boundaries where the elements are connected. The FEM provides a mathematical model based on subdividing the complete structure into smaller, easier to manage elements. [From 3]

The FEM does not provide an exact analytical solution. Some of the factors that effect accuracy of the FEM are element size, element type, and shape of element used. When dealing with approximations involving the sums of smaller pieces, the accuracy of the results is directly proportional to the number of elements used in the summation process. Small element size increases the number of summing pieces of the model and thus improves the model's accuracy. [From 4]

Elements can be one, two or three-dimensional. For two-dimensional elements, three and four sided elements like triangles, squares and rectangles are used. Three-dimensional elements are made from the same shapes as the two-dimensional cases except they have a thickness giving them five sides for triangular elements and six sides for the square and rectangular shaped elements. Elements that are uniform in shape provide better results regardless of whether they are two-dimensional or three-dimensional. To get the most accurate results, triangular shaped elements should be as close to equilateral triangles as possible while quadrilateral elements should be as close to squares as possible. Triangular elements are stiffer than quadrilaterals, so

their use should be minimized. Although FEM is an approximate solution, it is a powerful tool that can provide very accurate results and useful analysis when properly employed. [From 4]

B. COMPUTER SOFTWARE

1. IDEAS

In order to conduct an analysis, a finite element model must be created. For this analysis, the finite element model was created using version 6.0 of a computer program called IDEAS. IDEAS is developed and marketed by Structural Dynamics Research Corporation. It provides the user the ability to create structural models and mesh them for use in FEM analysis.

2. Dytran

Version 4.7 of MacNeal-Schwendler's Dytran analysis was used to provide the blast effects for this analysis. Dytran is a general purpose, three-dimensional program for simulating high-speed response of structures, and fluids. The program is designed to simulate and analyze extreme, short-duration events involving the interaction of fluids and structures, or problems involving the extreme deformation of structural materials. It is well suited for nonlinear dynamic or nonlinear quasi-static problems. It has the capability to perform finite element structural analysis, material flow analysis and coupled fluid-structure interaction with a single analysis package. [From 5]

To solve problems involving fluid flow and material displacement, like those seen in an explosion, Dytran makes use of both classic Eulerian and Lagrangian reference frames. An Eulerian mesh remains fixed in space while the fluid flows from one element to the next. In addition to this classic Eulerian technology, Dytran also offers an Arbitrary Lagrange Euler (ALE) algorithm. In ALE, the Eulerian mesh does not necessarily remain fixed in space, but moves relative to the material that is flowing through it. Both the Eulerian and ALE formulations in Dytran allow for the modeling of classic hydrodynamic materials like liquids and gases, as well as conventional structural materials such as steel. This latter capability provides a means of simulating structural response problems that are characterized by the extreme deformation of material, such as projectile impact/penetration. [From 5]

Dytran enables coupling of fluid-structure interaction. Dytran automatically and precisely calculates the physics of fluid-structure interaction by directly coupling the response of the Lagrangian finite element structural mesh and the Eulerian fluid flow mesh. In this approach,

pressure forces from the Eulerian flow mesh automatically load the structural finite element mesh at the boundaries between the Eulerian and finite element meshes via an automatic coupling algorithm. As the structural finite element mesh deforms under the action of the pressure forces from the Eulerian mesh, the resulting finite element deformation then influences subsequent material flow and pressure forces in the Eulerian mesh, resulting in automatic and precise coupling of fluid-structure interaction. A typical Dytran application involving fluid-structure coupling is structural response to internal bomb blast. [From 5]

Dytran's ability to model extreme, short-duration events where solid structure and fluids are coupled, make it an ideal choice for conducting computer based ballistic validation like that required for Comanche.

3. Patran

Patran, another MSC product, is an open-architecture, general purpose, 3D Mechanical Computer Aided Engineering (MCAE) software package with interactive graphics providing a complete CAE environment for linking engineering design, analysis and results evaluation functions. Post processing, or visualization of the simulated results derived by Dytran, was done using Version 9.0 of Patran for this analysis. Patran translates the numerical output from Dytran into a graphical representation. Patran can quickly and clearly display FEM analysis results in structural, thermal, fatigue, fluid, or magnetic terms. Patran displays time-dependent loads using multiple resultant color-coding on either deformed or undeformed geometry. Individual results can be sequenced in rapid succession to provide animation of the results. Additionally, Patran can be used to filter certain results and translate the results into other formats such as reports or graphs. [From 6]

C. BLAST MECHANICS

Immediately after the explosive round detonates, a spherical pressure wave radiates from the blast location. The energy from the explosion expands in the form of a spherical wave. As the pressure impacts on the surface of the tailfan shroud, part of the energy will be transferred to the structure while the remaining portion will reflect back into the blast area. The energy transferred to the structure will cause the structure to deform and the strain to increase. Additionally, the energy transferred to the structure excites responses in the structure causing it to

resonate in its normal modes. The high frequency responses dampen out more quickly as they translate through the structure, whereas the low frequency responses will remain. The low frequency responses will transfer energy to other portions of the structure and back into the blast area. The energy transferred back into the blast area will join the reflected blast energy and reflect around the structure to create additional deformation and strain changes in the structure. The reflecting energy forces the structure through a series of loading and unloading cycles. Over time the blast energy will either dampen out or be removed from the system through the pressure vents of the model. As time progresses, the pressures and strains in the model will become more uniform eventually returning to their pre-blast quasi-static state, with the exception of those highly loaded regions that experience permanent strain.

D. COMPOSITE MATERIALS

Composite materials are widely used in modern aircraft construction because they are light weight, yet provide high strength. Additionally, the designer is able to tailor areas to withstand specific loads by varying materials, material properties and fiber orientation. Structural composite materials, like those used in modern aircraft, consist of fiber-reinforced layers, or plies, impregnated with a resin that is then heat cured under pressure. The plies are added in various directions until the desired shape and strength is achieved. The plies are applied in different directions because the material usually has different properties for each direction and the structure must be capable of sustaining loads in different directions. The resin holds the various materials together while the heat is applied to cure the resin. Heat is applied along with pressure either by integrally heated tooling or by enclosing the specimen in an autoclave. Altering the type or amount of resin, or altering the time or temperature of the heating process, may change the properties of the composite material.

Suppose a composite fabric ply has a strength of 10,000 lbs/in in both of the normal directions, but no strength in the shear directions. If analysis indicates that the part needs to withstand 20,000 lbs/in in both the shear and both the normal directions, the part would need the combined strength of four plies to provide the required strength. Two of the plies must be aligned at 45° to provide strength in the normal direction and two plies must be aligned to provide strength in the shear direction. To ensure the plies are properly positioned, a reference direction, or 0° line, is selected. The reference direction is normally aligned with some feature or direction on the model. Rotating the plies designated to withstand loads in the shear direction at a 45°

angle relative to the plies designated to withstand the normal loads will ensure the proper strength is achieved in all directions. Assuming the 0° line is parallel to the x-normal direction, the plies might be placed in order at 0° , then 45° , then 0° again, then 45° again to get the required strength in each direction for this case.

The side skins of the tailfan shroud are comprised of Nomex honeycomb core with a composite skin bonded to each side of the honeycomb. Nomex honeycomb is a lightweight, series of small hexagonal cell structures that provide spacing between and stabilize the thin composite skins. The spacing between the skins offers greater structural stability through increased bending stiffness. The honeycomb opposes the shear forces transverse to the skin as well as the normal compression stresses. The skin facesheets oppose the in-plane and bending loads.

THIS PAGE INTENTIONALLY LEFT BLANK

III. MODEL DEVELOPMENT

A. OVERVIEW

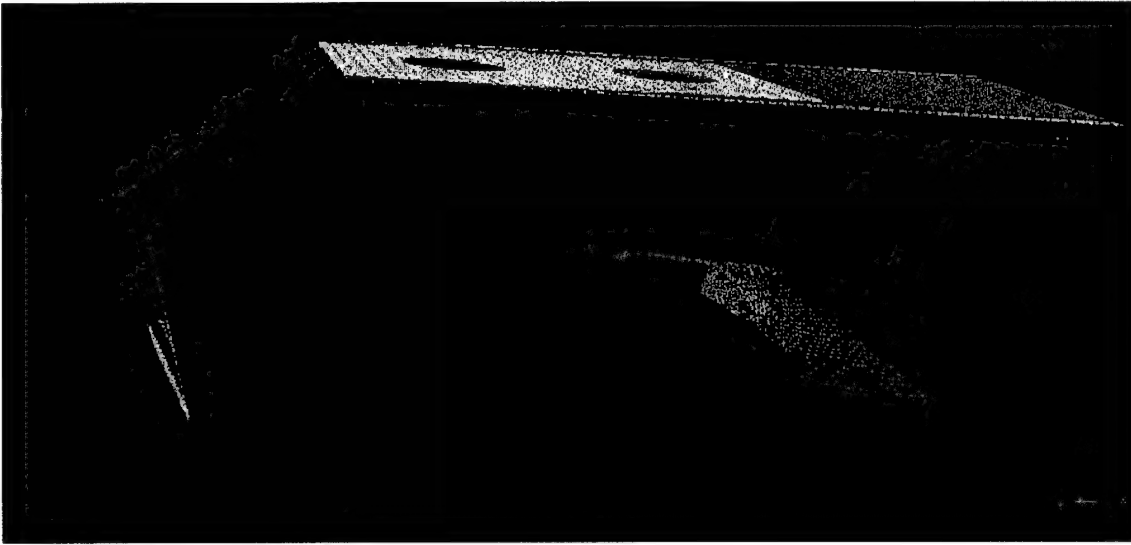


Figure 3: Left Side View of Model of Analysis Area

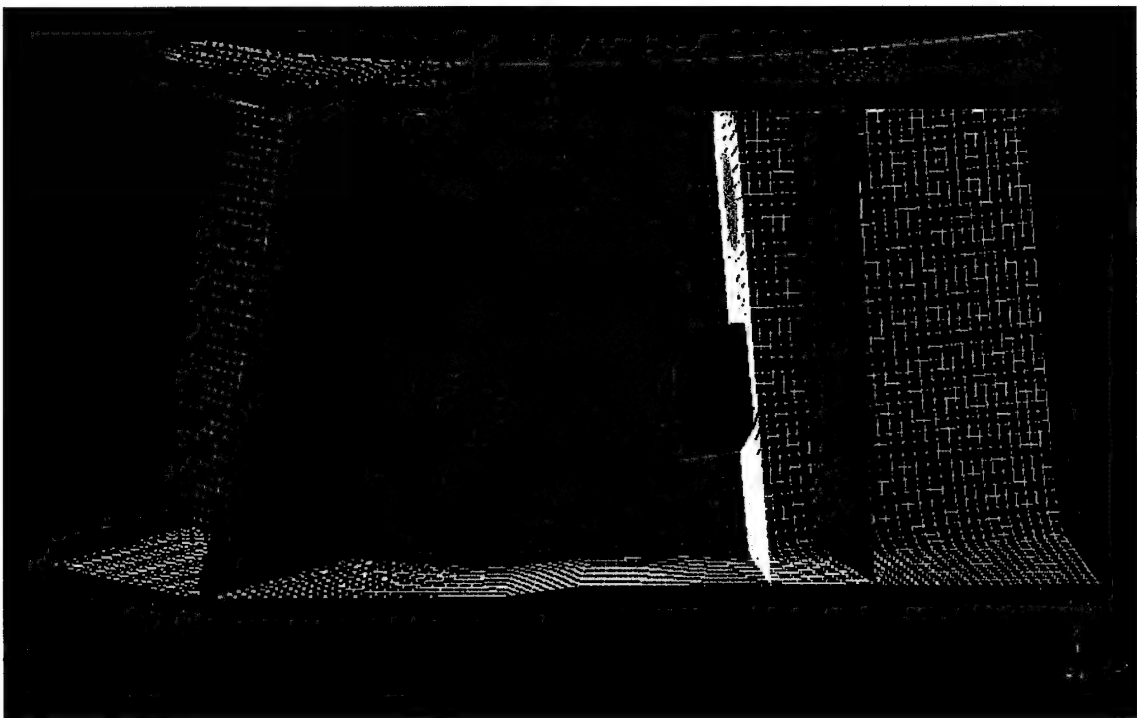


Figure 4: Top View of Model of Analysis Area with Top Plate Removed

The model of the analysis area is depicted in Figures 3 and 4. Figure 4 has the top plate removed in order to view the inside of the model. The varying colors are used to help organize the material properties of the model. The nose of the aircraft is to the reader's left in both figures.

As seen in Figures 3 and 4, the area includes three bulkheads, one fan strut, and a top plate. The primary materials used in construction of the tailfan shroud include: a composite made from graphite fabric, a composite known as Astroquartz, and honeycomb. The graphite is used to provide strength and stiffness to the structure. The inner face-sheet of the honeycomb skin, the bulkheads, fan strut and top plate are all made with graphite. Graphite is only used on internal structures because it has poor radar absorption properties. Astroquartz resists impact damage and is good for reducing radar signature, so it is used as the material for the outer face-sheet of the honeycomb panels. In addition to its structural stability, the honeycomb skin also helps reduce the vehicle's radar signature. For the shell elements making up the top plate and honeycomb panel skins in this model, the 0° reference line, or material coordinate x-direction, was set tangent to an arc running through the middle of the structure from front (closest to the nose) to rear. For the bulkheads and strut elements, the 0° reference line was set tangent to a line drawn from the bottom (closest to the tailfan) to the top on each surface. The 0° reference line is used to determine how the plies are oriented to make the various composite materials.

For this analysis, the top plate and fan strut are 0.1 inches thick, while the bulkheads are 0.2 inches thick. The inner and outer face-sheets that attach to the honeycomb are each .02 inches thick. Adhesives and fasteners that are used in final construction of the model are not currently represented in the model.

For the analysis in this report, the blast is detonated in the center of the box formed by the orange elements of Figures 3 and 4 and the first (Red in color) and second (Pink in color) bulkheads shown in Figure 4. While this area is the blast area, the model includes several inches of additional space on either side of the bulkheads to ensure that any constraints placed on the model do not affect the analysis.

Since an accurate model is the most important portion of any analysis, construction of the model was the most time consuming portion of the this project. Model construction was completed in the following phases: 1) CATIA Translation, 2) Part Cleanup, 3) Meshing, 4) Final Model Checks, 5) Dytran Translation.

B. CATIA TRANSLATION

All of the technical drawings of the Comanche at Boeing are made and stored using a program called CATIA. When approved, CATIA drawings go to the manufacturers who build the parts to the specifications in the drawing. CATIA is a drawing program that allows designers to design, edit and store technical drawings.

For this thesis, design drawings, which when finalized will be used to build the shroud around the tail fan, were collected. Portions of the drawings that did not relate to the area where the blast was originated were removed. The CATIA drawings show the dimensions and placement of all of the pieces that are used to construct the tail fan shroud. The model area has numerous pieces that fit together to make the component. CATIA data must be put into a FEM model in order to work with Dytran, so a translator program, which is part of the IDEAS program, was used to translate the CATIA drawings into IDEAS to build the FEM.

The various pieces or parts making up the area of analysis were translated from CATIA into IDEAS as simple volumes. After translation, the IDEAS parts had the same dimensions, orientation and spatial location as the CATIA parts which they were created from.

C. MODEL CLEANUP

Since the purpose of CATIA drawings is to show manufacturers how to build a piece, the emphasis in CATIA is making the part easy to build. Easily built parts do not necessarily translate into easily analyzed parts. In order to analyze parts effectively, they must be modified from a manufacturing configuration to an analytical configuration. Finite element analysis works best when the analysis is conducted on six sided, uniformly shaped solids. For an analytical configuration, the closer the part resembles a block, the better the analytical results. Since most items of interest are not block shaped, the modeler must make concessions in order to ensure the analysis can be performed. Minor details are adjusted from the manufacturing schematic in order to make the model easier to analyze. In particular, analyzing very small finite elements is difficult for the computer and requires much longer to process. To avoid these difficulties, a minimum distance between nodes of at least 0.4 inches is used. The 0.4-inch minimum value was determined by trial and error by Boeing. In their analysis, Boeing found that when nodes were much closer than 0.4 inches, the model took much longer to run and was more likely to fail. To

keep the elements above the 0.4-inch threshold, features that require small distances between nodes are altered or suppressed. Features are altered or suppressed only when changing them has an insignificant effect on the analytical results.

In this model, some common features that were changed include filleted (rounded) edges and pieces that taper to a sharp point. While these features are common in manufacturing because they are easy to work with, modeling them in finite element modeling requires very small distances between nodes. These types of features have an insignificant impact on a structural analysis; so modifying them into a more box-like shape helps the model produce better results without influencing the final outcome. To further simplify the model, large irregularly shaped pieces were broken down into smaller parts. The smaller parts are generally six-sided boxes that are easy for the computer to analyze. The end of this stage was all of the filleted edges and sharp tapering parts removed and the irregular shaped parts broken down into smaller six-sided box-like volumes. Modifying the model to this simpler configuration makes analysis simpler and faster than analyzing the model in its manufacturing configuration.

D. MESHING

Another big advantage of breaking large irregular shaped parts down into smaller six sided box-like shapes is that meshing the model is easier. With the model broken down into simple volumes, meshing is almost automatically done by IDEAS. The modeler just has to determine how many elements are desired along each of the three sides of the box. After picking an element size (0.4 inches in this case), the modeler just measures the side of interest and divides by the element size to get the number of elements along that side.

The model consists of solid and shell elements. Solid elements are 3-D (i.e. they have a length, width and thickness). The solid elements are used to replicate the honeycomb material in the model. Shell elements are 2-D elements that are used to replicate those items are very thin. The shell elements are used to replicate the skins attached to the honeycomb and flat plates like the bulkheads and strut. A combination of solid and shell elements provides the most accurate results.

When meshing with solid elements, the number of elements on opposing sides of the volume being meshed must be equal. Additionally, the number of elements on a side between two adjoining volumes that are being meshed must also be equal. Since the model component

has numerous curves and bends, uniform sized volumes was not always possible. In non-uniform volumes, meeting the requirements of equal elements on opposing sides was difficult. In these cases, transition elements like five sided volumes (triangular on each end with 3 sides) were used to complete the coverage of the structure with elements.

When modeling with 2-D shell elements, the best results are achieved by using 4-sided elements. When the component's shape prevents a good fit with 4-sided elements, triangular shaped elements are used as transition elements.

E. FINAL MODEL CHECKS

To complete the model and make it suitable for running on Dytran, several checks were made. The first and most important is the free edge check. The free edge check ensures that all of the elements fit together properly. Although the meshed model may look correct, tiny gaps, too small to see, may exist. Unwanted gaps in the model will corrupt the analysis and provide faulty data. To fix these problems, IDEAS identifies those element sides that are not touching other element sides. With the free edges identified, the modeler can fix any gaps that exist.

Each shell element has a front and a back. It is important that the fronts and backs of all elements in a section are pointed in the same direction. This is known as a connectivity check. For solid elements, the elements are grouped into one of three groups, x-normal, y-normal or z-normal. The direction pointing towards the inside of the model is the normal direction.

All of the composite materials need a reference direction in order to put the plies of material in the proper direction. Plies of material are laid in directions relative to the 0° reference angle in such a way to provide the required strength in all directions. The material orientation check assigns a 0° reference angle for each element. The 0° reference angle is set to be tangent to a curve that runs from the front (closest to the nose of the aircraft) to the back (closest to the tail of the aircraft) of the model.

The final check performed on the model was to renumber the elements. The elements were renumbered to sequentially list the elements by part. Renumbering ensures that no element numbers are skipped and makes setting up output requests for Dytran easier.

F. WRITING DYTRAN DECKS

Since the current version of IDEAS does not support input into Dytran directly, the IDEAS output is done in terms of Dytran's sister program Nastran. The Nastran output runs in Dytran with a few minor modifications. At this point, the location of the nodes and elements that make up the structural portion of the model are known, but the model is not complete. By manipulating the Dytran deck, the modeler must add the finite element mesh that represents the air surrounding the structure, associate material properties to the elements in the structure, and add the blast that simulates the detonation of the explosive round. After the finite mesh that represents the air is added, the modeler identifies contact points where the air and structure meet. These contact points allow Dytran to conduct coupling between the air and structural elements. Finally, the modeler selects the types and frequency of output required from Dytran in order to complete the analysis.

The modeler uses a series of computer commands, or cards, to communicate the required instructions to Dytran. Formats for each card are shown in the Dytran User's Manual. Adding a function into Dytran is as simple as copying the card format for the desired function out of the User's Manual and putting in the numbers as they pertain to the model being built.

IV. EXPERIMENTAL RESULTS

A. ASSUMPTIONS USED IN ANALYSIS

The results of this analysis are dependent upon the following assumptions:

- Dytran accurately models the characteristics of the explosions. Extensive testing of Dytran explosion analysis against real life explosions needs to be conducted in order to validate the Dytran output. To date, this comprehensive testing and comparison has not occurred. Boeing has begun an initial validation of this technique by attempting to correlate data from live-fire testing that was done on the static test article with computer simulations from Dytran. Additionally, Boeing is planning on conducting a live-fire test involving an explosion inside an instrumented test-box and comparing the results to the predicted results from the Dytran simulation.
- A complete, undamaged structure is present when the blast wave from the explosion impacts the structure. This assumption negates fragmentation damage, which is very difficult to predict. Fragments from the explosive round normally destroy or damage portions of the structure. If the structure is damaged or partially destroyed by fragmentation, it would most likely fail at lower stress/strain levels.
- Detonating a stationary, spherical charge at the center of the explosion area provides results similar to those achieved if an explosive round were in motion and exploded at any other point inside the box. With a relatively small explosion area, the pressure wave created by the explosion will not have an opportunity to dissipate before impacting the structure, so the same pressure and consequently the same damage will be seen regardless of where the round detonates in the blast area.
- The structure will catastrophically fail when 20% of its elements have failed. This simplifying assumption is a best guess of when the structure will catastrophically fail. Real life results may vary significantly.
- The materials used in construction are linearly elastic to failure. With this assumption, as elements exceed their ultimate strength, the element will break and no longer be capable of supporting the structure.

B. OVERVIEW

Six iterations of the model were run. The SIE for of the explosive round was the only parameter changed between runs. All of the runs used a stationary, spherical charge located at roughly the center of the box formed by the first and second bulkheads. The SIE values vary between 10^{10} and 10^{11} in²/sec².

Figure 5 shows the maximum, mid-plane ϵ_{xx} strain values by cycle for all six test cases. The ϵ_{xx} strain may not be the maximum strain seen by the system, but it is representative of the strain trends of the system. The geometric principal coordinates of the structural components do not necessarily coincide with the global coordinates. The x-direction for the coordinates on the structural elements is aligned with the 0° line used to align the material plies.

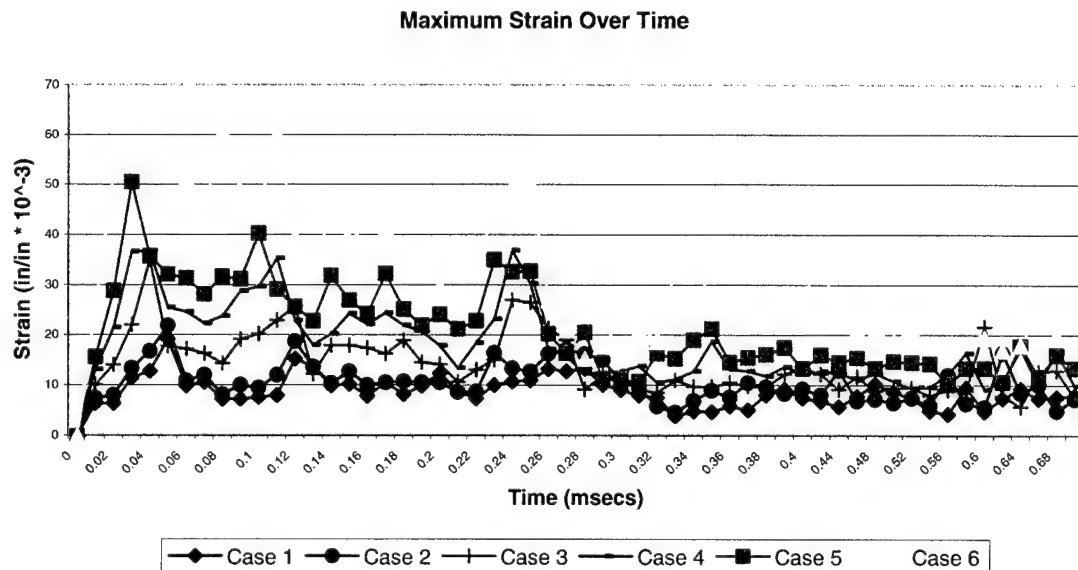


Figure 5: Plot of Maximum Strain vs. Time for All Test Cases

The graph shows that as the SIE values increase, the resulting maximum strains increase as well. Each of the test cases shows an initial spike in the strain followed by additional spikes that are usually smaller in magnitude. The decreasing trend in the strain spikes is primarily due to the venting of the blast wave over time. The initial strain spike is the blast wave impacting the structure for the first time. The smaller peaks are various energy waves reflecting around inside the structure. Some spikes in the model appear larger than the spikes that precede them. While the reflecting energy waves are not as strong as the initial wave, adding several reflecting waves

together can produce a resulting energy wave that is stronger than the initial blast. These out-of-sequence spikes are probably the result of multiple energy reflections converging at the same area at a given time.

The maximum strain from the initial shock wave appears at approximately the same area for each case. This area is indicated in yellow on the following picture:

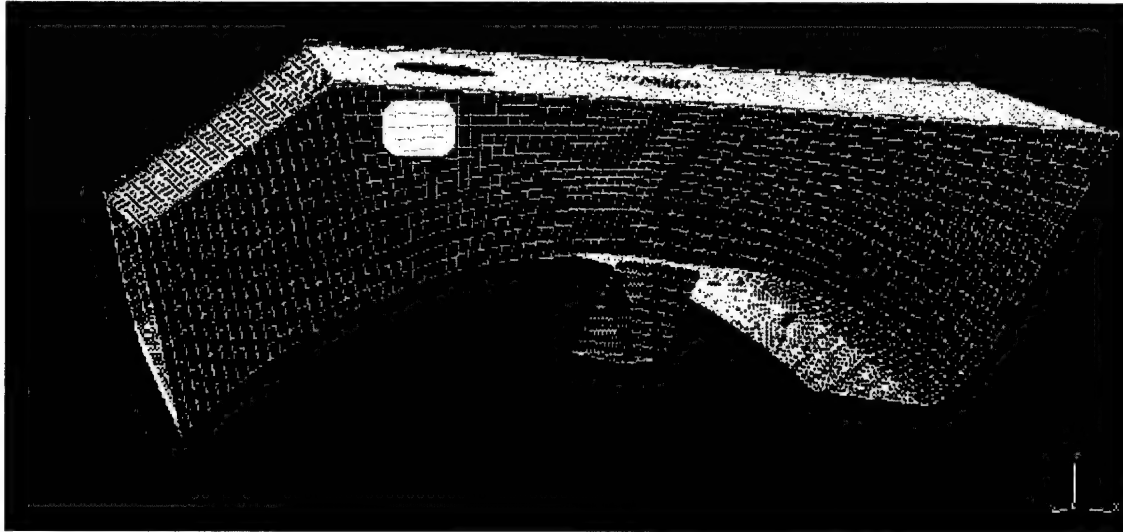


Figure 6: Maximum Strain Area from Initial Blast Wave

A picture of each of the result cases is shown in the following sections. The different colors indicate strain levels of varying magnitude as indicated by the scale on the side of each chart. The maximum strain for the initial blast is pictured for each result case. In most cases, the maximum strain from the initial blast wave is the absolute maximum strain level. Two pictures are shown for cases 3 and 6. The first picture is the maximum strain caused by the initial shock wave. The second picture in each case shows the absolute maximum strain for the test case.

C. TEST 1 RESULTS

MSC/PATRAN Version 9.0.01-Dec-0016:25:21

Fringe: Results #3, Cycle 905, Time 0.000500, EPSXX-MID,, (NON-LAYERED)

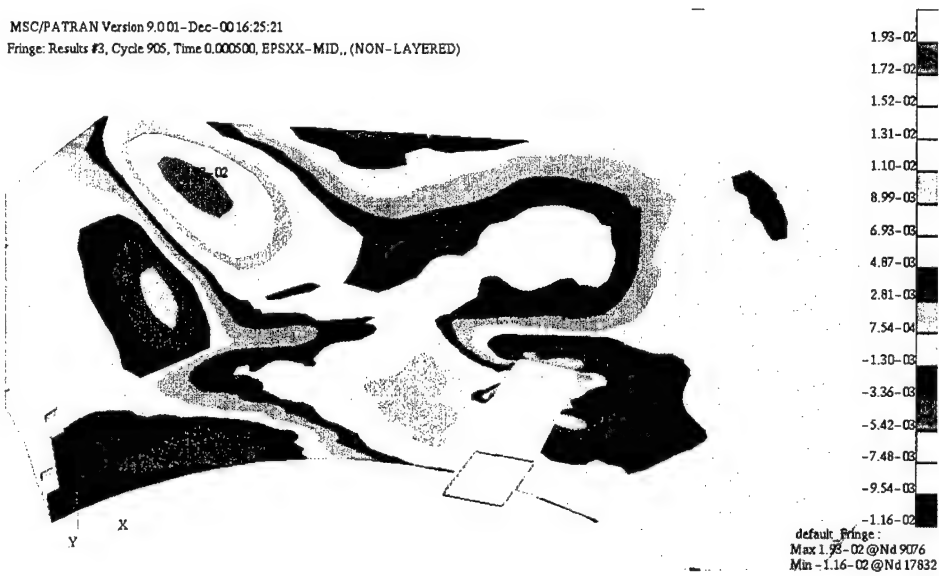


Figure 7: Maximum Strain for Test Case #1 ($SIE = 10^{10} \text{ in}^2/\text{sec}^2$)

D. TEST 2 RESULTS

MSC/PATRAN Version 9.0.01-Dec-0014:55:37

Fringe: Results #5, Cycle 905, Time 0.000500, EPSXX-MID,, (NON-LAYERED)

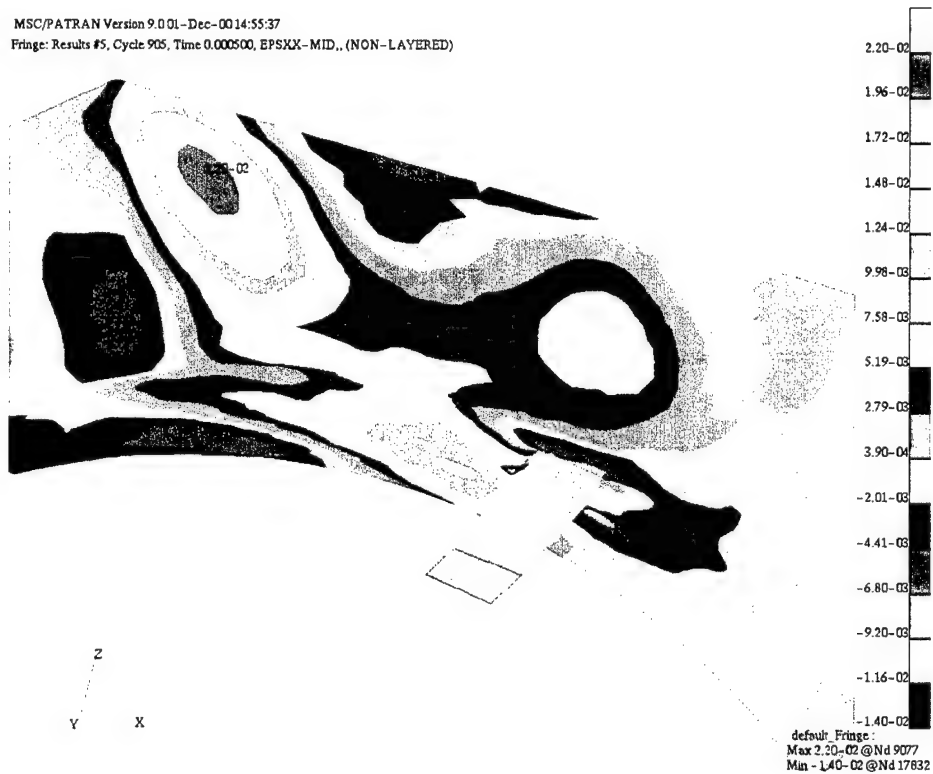


Figure 8: Maximum Strain for Test Case #2 ($SIE = 1.3 * 10^{10} \text{ in}^2/\text{sec}^2$)

E. TEST 3 RESULTS

MSC/PATRAN Version 9.0.01-Dec-00 15:47:19
Fringe: Results #5, Cycle 724, Time 0.000400, EPSXX-MID,, (NON-LAYERED)

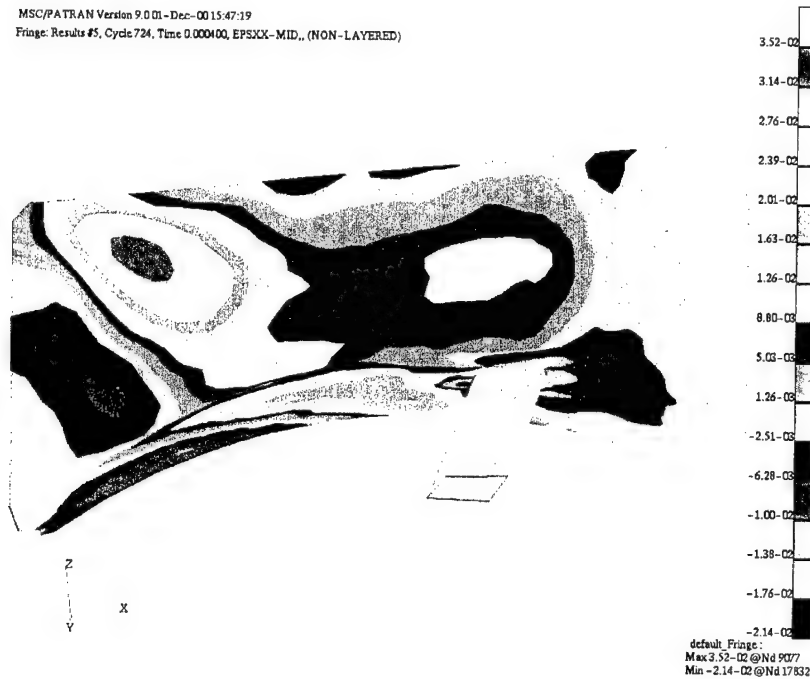


Figure 9: Maximum Strain for Test Case #3 ($SIE = 2.5 * 10^{10} \text{ in}^2/\text{sec}^2$)

F. TEST 4 RESULTS

MSC/PATRAN Version 9.0.01-Dec-00 16:14:04
Fringe: Results #5, Cycle 724, Time 0.000400, EPSXX-MID,, (NON-LAYERED)

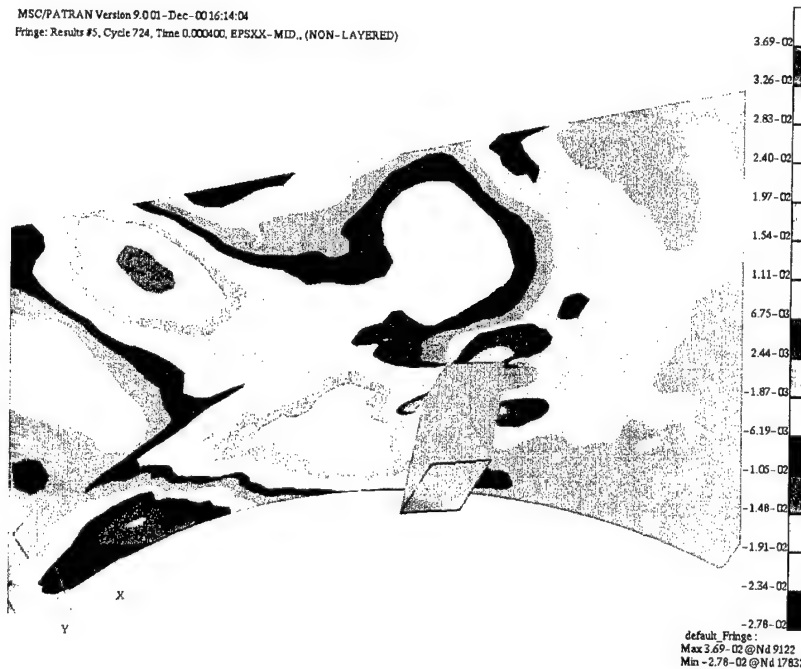


Figure 10: Maximum Strain from Initial Blast Wave for Test Case #4 ($SIE = 3.8 * 10^{10} \text{ in}^2/\text{sec}^2$)



Figure 11: Maximum Strain for Test Case #4 ($SIE = 3.8 * 10^{10} \text{ in}^2/\text{sec}^2$)

G. TEST 5 RESULTS

MSC/PATRAN Version 9.0.01- Dec-00 13:59:54
Fringe: Results #3, Cycle 543, Time 0.000300, EPSXX-MID,, (NON-LAYERED)
Deform: Results #3, Cycle 0, Time 0.000000, Displacement,, (NON-LAYERED)

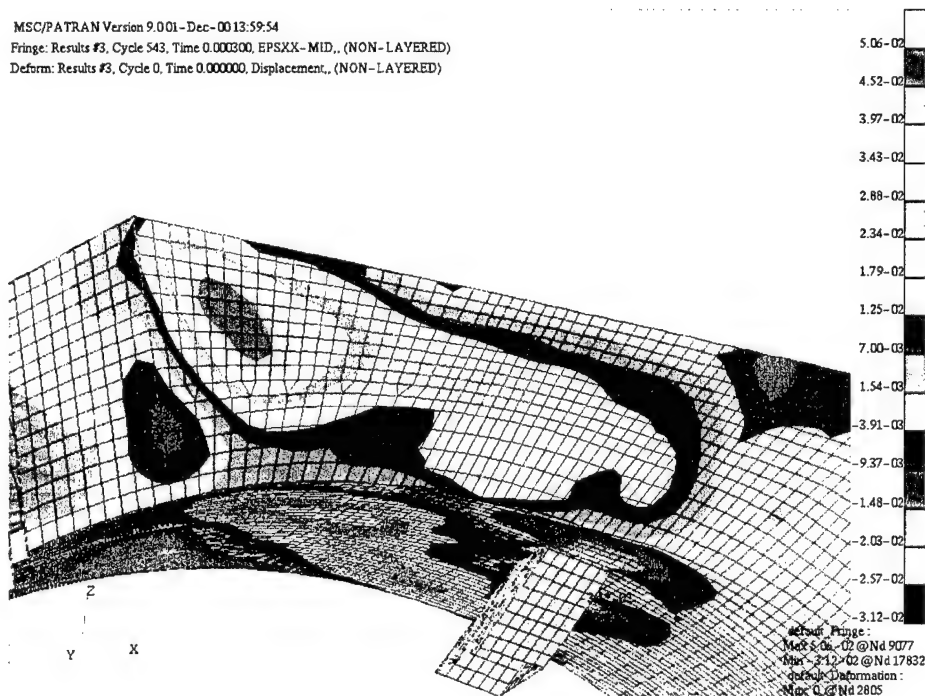


Figure 12: Maximum Strain for Test Case #5 ($SIE = 5 * 10^{10} \text{ in}^2/\text{sec}^2$)

H. TEST 6 RESULTS

MSC/PATRAN Version 9.013-Dec-00 13:56:15

Fringe: Results #4, Cycle 543, Time 0.000300, EPSXX-MID,, (NON-LAYERED)

Deform: Results #4, Cycle 0, Time 0.000000, Displacement,, (NON-LAYERED)

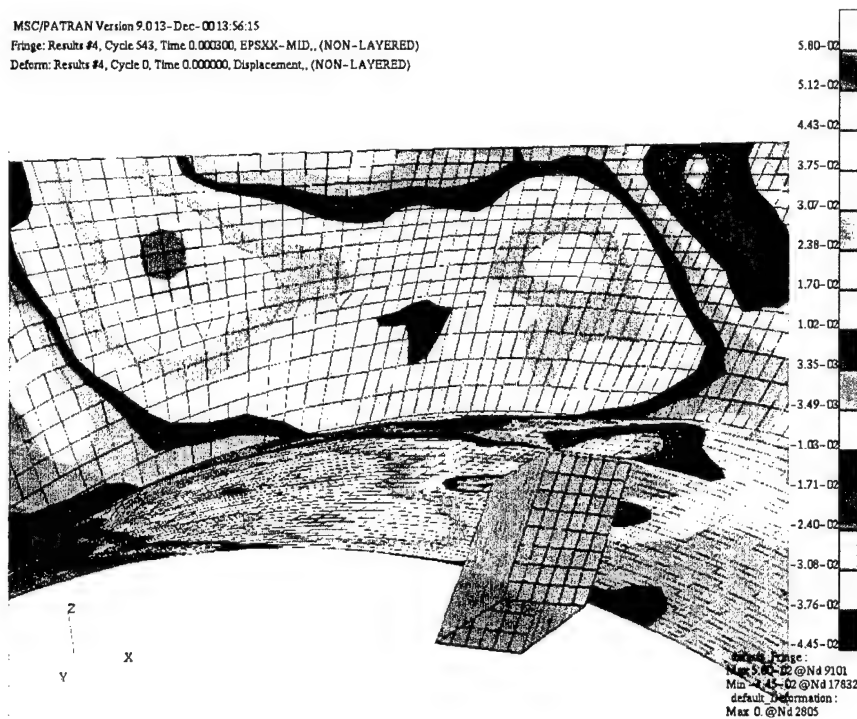


Figure 13: Maximum Strain from Initial Blast Wave for Test Case #6 ($SIE = 10^{11} \text{ in}^2/\text{sec}^2$)

MSC/PATRAN Version 9.013-Dec-00 13:58:04

Fringe: Results #4, Cycle 1448, Time 0.000800, EPSXX-MID,, (NON-LAYERED)

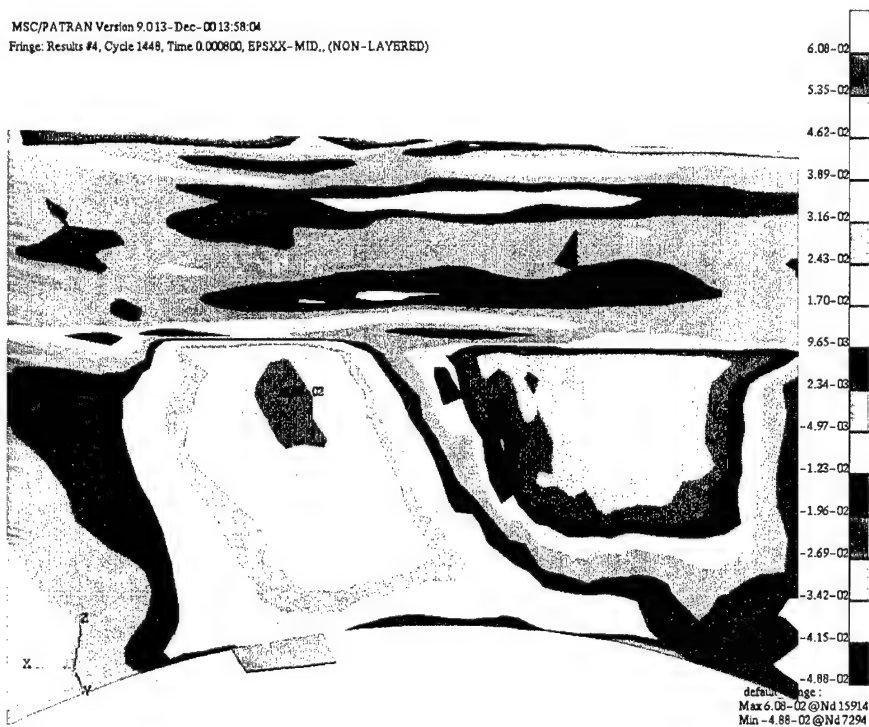


Figure 14: Maximum Strain for Test Case #6 ($SIE = 10^{11} \text{ in}^2/\text{sec}^2$)

I. MAXIMUM BLAST ENERGY STRUCTURE CAN WITHSTAND

The number of elements that failed for each blast level was noted. A failure is defined as any element exceeding the ultimate strain for that type of material. Strain is used to determine the allowable conditions instead of stress because strain provides more uniform results. Stress values may change significantly from layer to layer of composite materials, so the average stress may not accurately portray the actual loading conditions. Each element could only fail once. Once an element has failed for the first time, it is counted as a failure regardless of what else happens to it at later points in time. The mid-plane strain elements for all three loading cases (ϵ_{xx} , ϵ_{yy} , and ϵ_{xy}) were used to determine failures on the shell elements in the model. The mid-plane strain was selected because it provides the mean measurement of the true strain on each element. The number of failed elements for each run is listed in Table 1.

Run Number	SIE (in ² /sec ²)	Number of Failed Elements	Percentage of Total Elements Failed
1	$1.0 \cdot 10^{10}$	370	2.10
2	$1.3 \cdot 10^{10}$	777	4.42
3	$2.5 \cdot 10^{10}$	3,035	17.25
4	$3.8 \cdot 10^{10}$	5,836	33.16
5	$5.0 \cdot 10^{10}$	7,545	42.87
6	$1.0 \cdot 10^{11}$	10,659	60.57

Table 1: Failure Data for Each Cycle

The data from Table 1 is plotted in graphical form in Figure 15 on the following page.

Percent Failure vs. Blast Strength

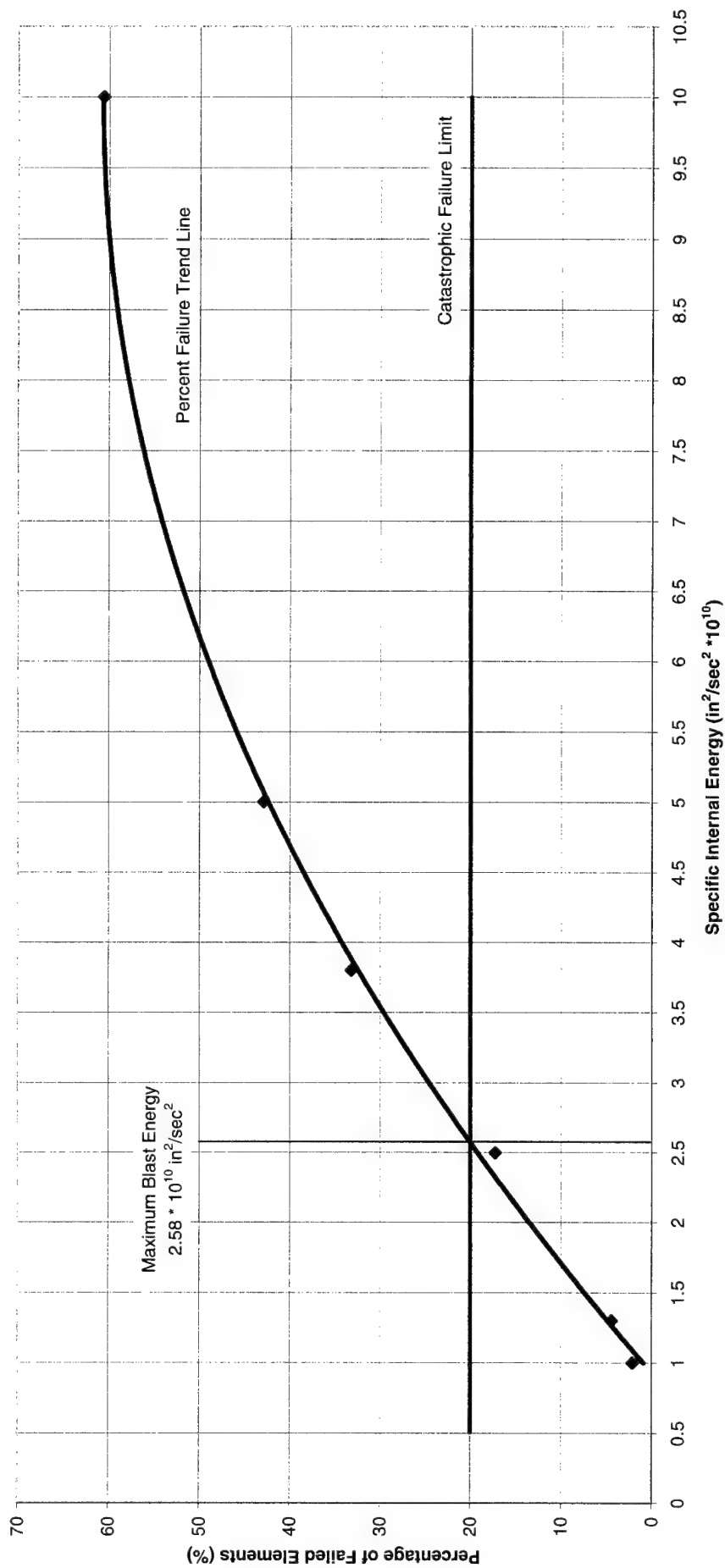


Figure 15: Plot of Percentage of Failed Structure vs. SIE

In Figure 15, the blast level in SIE is shown on the X-axis, while the Y-axis shows the percentage of total elements that fail. The actual percentages of failures for the six test cases are indicated as diamonds on the graph. The trend line curve indicated on the graph is a best-fit curve derived from a 2nd order polynomial analysis of the six data points. The chart indicates a catastrophic failure line where 20% of the total elements fail. This 20% is an arbitrary point picked by Boeing as an approximation of when a catastrophic failure would most likely occur. A catastrophic failure is a failure where the aircraft would no longer be flyable after sustaining this type of damage. Using the 20% failure criterion as the catastrophic limit, the point where the failure trend line and Catastrophic Failure line cross is the maximum amount of blast energy the test section can withstand and remain flyable. The line drawn at $2.58 \times 10^{10} \text{ in}^2/\text{sec}^2$ shows the maximum blast energy that the structure can withstand.

V. CONCLUSIONS AND RECOMMENDATIONS

A. CONCLUSIONS

Based on assumptions made during this analysis, the section of the tailfan shroud analyzed in this report can survive a hit from an explosive round with a SIE of $2.58 * 10^{10}$ in²/sec².

B. RECOMMENDATIONS

The maximum sustainable value of $2.58 * 10^{10}$ in²/sec² should be compared to the SIE values of the various explosive rounds that may be used against the Comanche. Those rounds with SIEs higher than $2.58 * 10^{10}$ in²/sec² should be classified as capable of causing a catastrophic failure on the aircraft if they explode within the area of structure analyzed in this report.

Combine the results of this analysis with similar analysis on other portions of the aircraft to obtain a picture of how survivable the entire aircraft is to ballistic damage. For this type of analysis, a standard round should be selected and applied to all areas. Those areas that experience a catastrophic failure when struck by the designated round should be identified as risk regions.

After the ballistic survivability for the entire aircraft is determined, a trade study should be conducted to determine if it is feasible to make the aircraft more ballistically survivable. Increasing the structural stiffness in risk regions will increase the aircraft's ballistic survivability. Unfortunately, increasing the stiffness generally increases the aircraft weight and in turn reduces the aircraft's performance. Careful analysis must be conducted on all potential improvements to ensure the survivability improvements are justifiable given the adverse effects they would most likely cause on weight, performance and cost.

Comprehensive testing of the Dytran results is required to validate this technique. If the results of Boeing's initial correlation efforts appear promising, the Army, as the ultimate beneficiary of this testing procedure, should conduct a comprehensive evaluation of the capabilities of this type of analysis for application towards Army standards. Until this computer modeling technique can be shown to provide accurate results, the Army test community will not accept the results generated from this type of analysis. Consequently, to achieve satisfactory

validation it may be necessary to destroy a higher number of components than desired in live-fire testing. This type of testing is very costly. It is extremely important to direct a major effort at computer modeling of ballistic testing. If it can be accomplished and show the same accurate results as current live-fire testing methods, additional money and time will be saved and made available to the program.

It follows that a successful computer based ballistic modeling program will lead to better, cheaper products. The ability to accurately test designs before they are built will allow designers to analyze numerous potential designs, identify shortcomings and fix problem areas early in the design process, before wasting resources on manufacturing components that do not work. Additionally, the money and time saved over conventional ballistic testing methods could be applied to improve other areas of the program.

LIST OF REFERENCES

1. <http://www.boeing.com/rotorcraft/military/rah66/rah66photos.htm>
2. <http://www.boeing.com/rotorcraft/military/rah66/>
3. Allen, David H. and Haisler, Walter E., *Introduction to Aerospace Structural Analysis*, John Wiley and Sons Inc., New York, New York, 1985.
4. Brauer, John R., *What Every Engineer Should Know about Finite Element Analysis*, Marcel Dekker, Inc., New York, New York, 1988.
5. <http://www.compumod.com.au/products/dytran/dytran.htm>
6. <http://www.compumod.com.au/products/patran/patran.htm>
7. Tobin, Vincent M., *Analysis of Potential Structural Design Modifications for the Tail Section of the RAH-66 Comanche*, Master's Thesis, Naval Postgraduate School, Monterey, California, June 1997.
8. MacNeal-Schwendler Corporation, *MSC/DYTRAN User's Manual*, Version 4.7, 1997.

THIS PAGE INTENTIONALLY LEFT BLANK

INITIAL DISTRIBUTION LIST

1. Defense Technical Information Center 2
8725 John J. Kingman Road, Suite 0944
Ft. Belvoir, VA 22060-6218
2. Dudley Knox Library 2
Naval Postgraduate School
411 Dyer Road
Monterey, CA 93943-5101
3. Department of Aeronautics and Astronautics, Code AA 2
Naval Postgraduate School
411 Dyer Road
Monterey, CA 93943-5101
4. Professor E. Roberts Wood, Code AA/WD 2
Department of Aeronautics and Astronautics
Naval Postgraduate School
Monterey, CA 93943-5101
5. Professor Donald A. Danielson, Code MA/DD 2
Department of Mathematics
Naval Postgraduate School
Monterey, CA 93943-5101
6. CDR Mark A. Couch, Code AA/CM 1
Department of Aeronautics and Astronautics
Naval Postgraduate School
Monterey, CA 93943-5101
7. COL Robert P. Birmingham, Project Manager RAH-66 1
Building 5681 Wood Road
Redstone Arsenal, AL 35898
8. MAJ (P) Vincent M. Tobin, APM, Test and Evaluation..... 1
Building 5681 Wood Road
Redstone Arsenal, AL 35898

9. Mel Niederer, Boeing Helicopter Structural Engineer..... 1
Building 325, Gate 6 (Stewart Avenue and Industrial Avenue)
Ridley Park, PA 19078
Mail Stop P10-74
10. CPT Allen Stephan..... 1
12713 Water Point Blvd.
Windermere, FL 34786